Formulation of a Physically Motivated Specific Breakage Rate Parameter for Ball Milling via the Discrete Element Method

Maxx Capece, Ecevit Bilgili, and Rajesh N. Davé
Otto H. York Dept. of Chemical, Biological, and Pharmaceutical Engineering, New Jersey Institute of Technology, Newark, NJ 07102

DOI 10.1002/aic.14451
Published online April 1, 2014 in Wiley Online Library (wileyonlinelibrary.com)

A physically based specific breakage rate parameter of the population balance model for batch dry-milling is formulated, which explicitly accounts for the impact energy distribution calculated by the discrete element method (DEM). Preliminary DEM simulations of particle impact tests were first performed, which concluded that dissipation energy should be used in contrast to collision energy to accurately define the impact energy distribution. Subsequently, DEM simulations of the motion of spheres representing silica glass beads in a ball mill were performed to determine the specific breakage rate parameter, which was in good agreement with those found experimentally. An analysis of the impact energy distribution, which was only possible within context of the physically motivated specific breakage rate parameter, emphasized the importance of accounting for a threshold impact energy. Without proper assessment of the impact energy distribution, DEM simulations may lead to an erroneous evaluation of milling experiments. © 2014 American Institute of Chemical Engineers *AIChE J*, 60: 2404–2415, 2014

Keywords: discrete element method, population balance model, batch dry milling, breakage rate parameter, particulate process

Introduction

Milling for the purpose of particle size reduction is a pervasive and enduring unit operation used across a variety of industries including the mineral, pharmaceutical, food, pigment, and ceramic.[1] Despite the importance, milling processes are still poorly understood in part due to the absence of constitutive equations derived from first principles used to describe particle fracture. Consequently, milling processes are difficult to design, control, and scale up as is often the case with other types of particulate processes (e.g., blending or packing). Phenomenological modeling tools are, therefore, crucial to gain fundamental understanding of this complex process. Population balance modeling (PBM) is one such tool extensively used to mathematically describe and analyze milling processes.[2]

PBMs applied to milling processes describe the spatio-temporal variation of the particle-size distribution (PSD) and can be used to determine mill performance as well as identify the breakage mechanism of particles (e.g., fracture, cleavage, and attrition).[3] PBMs are also commonly used for control and optimization.[4] For a well-mixed batch milling process, the general size-discrete linear PBM, which describes milling as a first-order rate process is given in Eq. 1[2]

$$\frac{dm_i(t)}{dt} = -k_i m_i(t) + \sum_{j=1}^{i-1} b_{ij} k_j m_j(t) \tag{1}$$

where $m_i(t)$ is the mass fraction of particles with size x_i in size class i at milling time t. The first term on the r.h.s. is the death or disappearance rate at which particles of size x_i are broken into smaller particles. The second term on the r.h.s. represents the summed rate at which particles in all size classes $j < i$ are broken into size class i, where i and j are size class indices extending from size-class 1 containing the coarsest particles to size class N containing the finest particles usually in a geometric progression. k_i is the first-order specific breakage rate (selection) parameter and describes the propensity for a particle to break. b_{ij} is the breakage distribution parameter, which describes the mass fraction of particles formed in size class i when particles in size class j are broken.

The PBM of Eq. 1 is a powerful tool used to determine the evolution in PSD for batch milling processes. The parameters k_i and b_{ij} must be obtained by experiments. Typically, this task is accomplished by laborious direct measurements on the breakage of narrowly sized feeds or by fitting experimental milling data from one or preferably multiple milling experiments with Eq. 1.[5,8,9] In both cases, size-dependent empirical functions are chosen to accurately describe the specific breakage rate parameter and the breakage distribution parameter for all particle sizes under consideration.[8] However, such functions are devoid of any consideration of fundamental physics of particle breakage, that is, fracture mechanics and statistical nature of occurrence and distribution of flaws.[9,10] Furthermore, these parameters are dependent on a combination of material properties and milling process conditions, which make the predictive capability of the PBM problematic when considering

Correspondence concerning this article should be addressed to R. N. Davé at dave@njit.edu.

different materials, conditions, or types of mills. Consequently, there is necessity to define these parameters considering the physics of mechanical interparticle interactions and particle breakage at the microscale.

While PBM allows a description at the process length scale, recent work has focused on modeling the milling process through particle scale phenomena to improve on the "gray-box" nature of the PBM.[11–15] At the microscale, particle size reduction is simply the result of a succession of mechanical interactions between the feed material, grinding media, and vessel geometry. At the macroscale, these interactions produce complex granular flow and particle fracture behavior, which are difficult to resolve. Particle scale interactions are challenging to observe and quantify experimentally in a typical mill, which leaves numerical modeling schemes such as the discrete element method (DEM) as one of the few techniques able to provide the necessary microdynamic information.[16–19] DEM determines the trajectory and interaction of discrete particles using Newton's second law of motion combined with well-established contact mechanics models, which can simulate the behavior of a wide range of particulate processes including milling.[20,21]

Initial DEM studies were primarily qualitative comparisons between simulated and experimentally observed granular motion in a mill, but demonstrated the method's validity.[19–21] Recently, the method has rapidly developed to relate the milling performance and breakage rate via simulation of particle interactions obtained by DEM.[11–15,22–28] However, there are many issues and caveats in this approach that must be addressed, which will be elaborated below. Since the fundamental phenomenon for particle breakage occurs due to a stress-induced event such as a collision of a feed particle with grinding media, most studies have sought to relate the impact energy distribution obtained from DEM simulations to the breakage rate.

Determination of the specific breakage rate parameter in the context of DEM, which is of primary concern in this current study, has followed several approaches. The most straightforward approach simply seeks to correlate an experimentally determined breakage rate parameter to the total or average impact energy associated with the collision of grinding media obtained from DEM simulations.[22–25] The breakage rate parameter determined in these particular studies are unrelated to k_i of Eq. 1, but is indicative of milling efficiency as it does describe the rate at which size reduction occurs. While these studies concisely demonstrate the relationship between milling behavior and particle interactions obtained from DEM, they do not isolate material properties from the milling environment nor do they include any fundamental considerations for particle breakage. Consequently, these studies are limited in any predictive capacity including the inability to determine the PSD, which can only be obtained via solution of Eq. 1. An enhanced approach introduced by Datta and Rajamani[11] sought to determine the specific breakage rate parameter of Eq. 1, which is a significant improvement over the aforementioned studies. The method used by Datta and Rajamani[11] correlates the impact energy to a broken mass of particles, which is experimentally determined from powder bed drop-ball tests. A breakage rate is then defined as the total mass of particles broken due to each collision whose energy and frequency is determined by DEM. Despite the developments of Datta and Rajamani,[11] their approach also does not consider fundamental particle breakage behavior and may be limited in the case when milling dynamics deviate from the idealized powder bed breakage tests. In addition, various assumptions were made related to the distribution of the impact energy to feed particles in the mill since their DEM simulations only included grinding media. Wang et al.[12] expanded on the work of Datta and Rajamani[11] by simulating both grinding media and feed particles. However, both approaches also used the impact energy distribution by assuming that impacts of all energies contribute to breakage, which is not a reasonable assumption since single particle impact tests have shown that a minimum impact energy must be overcome to cause defects or crack propagation for particle breakage to occur.[9,10] Furthermore, particles may store defects and become weaker due to impacts insufficient to cause outright breakage but may break after a succession of impacts.[9,10] These points stress the importance and necessity of particle breakage models based on fracture mechanics considerations if microdynamic information is to be used to predict or quantify particle breakage.

This study addresses the use of particle scale interactions obtained from DEM to determine the specific breakage rate parameter of the PBM for batch dry milling. As a major novelty, the current study properly formulates for the first time, a physically motivated specific breakage rate parameter based on a particle breakage model derived by Vogel and Peukert[9,10] using fracture mechanics considerations. The physically motivated specific breakage rate parameter is referred to as such because it explicitly accounts for the phenomenon of particle breakage as a result of a stressing event or external load. Further, novelty in the specific breakage rate parameter is due to the fact that it also separates the contribution of material properties from the milling environment, which is defined by the impact energy distribution obtained by DEM. Currently, there is no specific breakage rate parameter that is explicitly expressed in terms of impact energy and material parameters that has been properly related to the PBM for batch milling. In this study, preliminary DEM simulations of particle impact tests were performed, which concluded that energy dissipated at impact (i.e., deformation energy) is preferable to the collision energy to accurately define the impact energy distribution. Next, DEM simulations of spheres representing silica glass beads processed in a rolling ball mill were performed to determine the motion and mechanical interactions between the feed, media, and mill geometry. The specific breakage rate parameter was determined from DEM simulations and compared to the specific breakage rate parameter obtained by milling experiments under different processing conditions. In contrast to most studies, both the feed material and the grinding media were simulated to obtain the most accurate impact energy distribution. As will be shown, the specific breakage rate parameters determined by DEM simulations were in close agreement with experimental results confirming the validity of the proposed methods. As another major novelty, analysis of the milling environment defined by the impact energy distribution was performed within the context of the physically motivated specific breakage rate parameter introduced here. The analysis is intended to emphasize the importance of accounting for a threshold impact energy to identify which impacts do not contribute to particle breakage and hence should not be included in the analysis. Neglecting to account for a threshold impact energy may lead to an erroneous interpretation of milling simulations. Thus, the

overall objective of this study is to demonstrate that DEM can quantify particle scale interactions and their impact on the specific breakage rate parameter of the PBM for batch dry milling, in particular, when a threshold impact energy is taken in to consideration. More importantly, this study is expected to contribute to the development of a unified DEM–PBM framework with a physically motivated specific breakage rate parameter, which will lead to better design, optimization, control, and mechanistic understanding of dry milling processes.

Theoretical Development: A Physically Motivated Specific Breakage Rate Parameter

The typical milling process is extremely complex and influenced by mill geometry/size, mill speed, lifter configuration, grinding media size/density, feed size/density/mechanical properties, fractional loading of grinding media/feed, just to name a few. These operating parameters affect the individual particle interactions, which are responsible for bulk granular motion, the size reduction rate, breakage mechanism, product size, and size distribution. Consequently, this section focuses on defining a specific breakage rate parameter for batch dry milling processes, which can be determined from particle scale interactions obtained by DEM simulations.

Because of the complexity of particle ensembles, single particle impact tests are excellent for fundamental study of particle breakage. In one such study, Vogel and Peukert[9] studied the breakage of various materials including glass, limestone, and polymers subjected to single particle impacts of varying energy and derived an equation for their breakage probability. The derived equation given in Eq. 2 was based on fracture mechanics considerations using Weibull statistics for breakage probability introduced by Weichert (see Ref. 9) and a similarity analysis originally developed by Rumpf,[29] which took into account various concepts including crack initiation/propagation, pressure distribution (i.e., Hertz's elastic theory), and stress due to particle deformation

$$P_{\mathrm{B}} = 1 - \exp\left[-f_{\mathrm{Mat}}\, x M \left(E_{\mathrm{m}} - E_{\mathrm{m,min}}\right)\right] \tag{2}$$

here P_{B} is the breakage probability of a particle subjected to an external load or stress event such as a collision with a mass-specific energy E_{m}. x is the particle diameter and M is the number of impacts experienced by a particle. The term $M(E_{\mathrm{m}} - E_{\mathrm{m,min}})$ is the total impact energy by one or a succession of impacts that a particle is subjected to which may cause fracture. As the total energy increases, the breakage probability of a particle increases from 0 to a maximum of 1. The two material properties, f_{Mat} and $E_{\mathrm{m,min}}$, are respectively referred to as the material strength parameter and the threshold energy. The former denotes a material's resistance against fracture under an external load and takes into account the particle's relevant fracture and deformation mechanical parameters. The latter is also a material property, which gives the energy that must be surpassed to initiate fracture either through single or multiple impacts. Below this energy threshold, fracture will never occur regardless of the number of stress events.[9,10] Since both the strain energy that can be stored within a particle and number of preexisting flaws depend on its volume, $E_{\mathrm{m,min}}$ must be dependent on particle size. While $E_{\mathrm{m,min}}$ is a size-dependent material property, Vogel and Peukert[9] determined that the product $xE_{\mathrm{m,min}}$ is a constant material property.

In the experiments of Vogel and Peukert,[9] particles were subjected to a single collision with predetermined collision energy provided by an impacting plate. In a typical milling process (e.g., rolling ball mill), a particle will undergo a large succession of impacts each with a different impact energy in a given amount of time. To make Eq. 2 compatible with this type of milling environment, a modified form is presented in Eq. 3

$$P_{\mathrm{B}} = 1 - \exp\left[-f_{\mathrm{Mat}}\, x \sum_{l=1}^{L} f_{\mathrm{coll},l}\left(E_{\mathrm{m},l} - E_{\mathrm{m,min}}\right) t\right] \tag{3}$$

here the total impact energy is $\sum_l^L f_{\mathrm{coll},l}(E_{\mathrm{m},l} - E_{\mathrm{m,min}})t$ where $f_{\mathrm{coll},l}$ is the collision frequency and $f_{\mathrm{coll},l}\, t$ is the total number of impacts with energy $E_{\mathrm{m},l}$ occurring within the milling time t. A mass-specific energy rate $\dot{E}_{\mathrm{m}}$ can also be defined as $\sum_{l=1}^{L} f_{\mathrm{coll},l}(E_{\mathrm{m},l} - E_{\mathrm{m,min}})$. For ease of data processing with DEM simulations in this study, impact energy has been discretized into L number of bins. A similar equation was also used by Bruchmuller et al.[26] in DEM simulations investigating the particle breakage distribution of particles resulting from fracture. The major difference here is the consideration of collision frequency and milling time due to the time-continuous nature of the batch milling processes considered here. This is opposed to the impact tests of Vogel and Peukert,[9] which do not explicitly involve time, but repeated stressing events. Thus far, Eq. 3 can be used to determine the breakage probability of a single particle undergoing repeated stressing events in a mill provided that the impact energy distribution can be resolved from DEM simulations. Breakage probability is also equivalent to a broken fraction (i.e., the mass fraction of particles smaller than the initial feed size) if considering a large number of particles in which it is assumed that all particles are also subjected to the same impact energy distribution. It should also be noted that Eq. 2 and, as an extension, Eq. 3 have only been examined with respect to impact milling that results in particle fracture as shown by Vogel and Peukert.[9,10] The validity of the model with respect to shear-based milling processes resulting in abrasion or attrition is unknown.

Although breakage of a single particle is indeed a statistical event warranting the use of a breakage probability, the breakage of an ensemble of particles is more appropriately described as a rate for time-dependent milling processes.[30,31] The former case is most relevant for milling processes with short retention times, which produce a small number of stressing events such as roller milling, hammer milling, or single impact tests as described above. The latter case refers to long retention-time type mills such as ball mills, which are considered here. In this work, we also seek a definition of the specific breakage rate parameter explicitly based on impact energy distribution analogous to the breakage probability of Eqs. 2 and 3. This can be accomplished by relating the breakage probability to the specific breakage rate parameter. The treatment detailed by Vervoorn and Austin[32] is used in the following and their procedure is reproduced in the following with only slight modification.

We first consider a time-dependent batch milling process, which can be described by Eq. 1. In this case, a mono-sized feed is considered, which allows disregard of the second term on the r.h.s. Solving Eq. 1 under these assumptions yields the well-known solution for the variation in the mass fraction of material left unbroken $m_i(t)$ with time as shown in Eq. 4

$$m_1(t) = m_1(0)\exp\left(-k_1 t\right) \tag{4}$$

Here we only consider the top-most size class ($i=1$) which represents that of the mono-sized feed. Next, we consider the grinding time t to be equivalent to N stages or intervals of milling each with a duration of Δt ($t=N\Delta t$), which allows Eq. 4 to be written as

$$m_1(N)=m_1(0)\exp\left(-k_1 N\Delta t\right) \tag{5}$$

If we consider one stage of milling ($N=1$) and use the definition for breakage probability, $P_B=1-m_1(1)/m_1(0)$, we arrive at

$$P_B=1-\exp\left(-k_1\Delta t\right) \tag{6}$$

Equation 6 gives the relation between the specific breakage rate parameter and breakage probability, and we note the equivalency in the form of Eq. 3 if a small milling time Δt is also considered. Noting this equivalency, we finally arrive at the equation for an energy-based specific breakage rate parameter given in Eq. 7

$$k\equiv k_1=f_{\mathrm{Mat}}\,x_1\sum_{l=1}^{L} f_{\mathrm{coll},l}\left(E_{\mathrm{m},l}-E_{\mathrm{m,min}}\right) \tag{7}$$

The derivation here is distinctly different from the specific breakage rate parameter previously formulated by Concas et al.[15] who defined k in an *ad hoc* approach as the product of collision rate and the breakage probability of Eq. 2 neglecting to note the relationship between breakage probability and the specific breakage rate parameter as shown in Eq. 6. Similar to Datta and Rajamani,[11] Concas et al.[15] also made assumptions related to the mass of feed captured in each impact due to the fact that only the grinding media were simulated in DEM. Concas et al.[15] also used average collision energy and collision frequency to determine the specific breakage rate parameter. These deficiencies in determining the specific breakage rate parameter and analysis of milling process exemplified by the study of Concas et al.[15] and characteristic of similar studies[11–15,22–28] are resolved here by use of Eq. 7. The formulation of the physical specific breakage rate parameter accounts for the contribution of each and every impact on feed particles and thus does not require any assumption based on the mass of particles captured in each collision.

Equation 7 allows determination of the specific breakage rate parameter based on the impact energy distribution provided by DEM simulations. The specific breakage rate parameter is traditionally found by milling various mono-sized or narrowly distributed feeds, measuring the disappearance of the feed due to breakage, and fitting Eq. 4 to the experimental data.[5] Following the methodology of experimentalists, DEM simulations can be performed with various mono-sized feeds for which the specific breakage rate parameter is determined for each particle size by use of Eq. 7. It is important to note that determination of the specific breakage rate parameter does not yield the particle breakage rate or evolution of the PSD since the proposed method do not involve breakage of particle in DEM simulations. However, once the specific breakage rate parameters are obtained, the PBM of Eq. 1 can be solved to determine the actual breakage rate and the PSD for any milling time assuming first-order breakage kinetics remains valid. The breakage distribution parameter must also be known and can be determined by experimental measurement and fitting,[1,6–8] but discussion of physically based breakage distribution parameter is outside the scope of this study. Typically, the specific breakage rate parameter of Eq. 1 is a size-dependent empirical function with no physical relevance.[5,8] In contrast, the specific breakage rate parameter of Eq. 7 is a powerful formulation as it explicitly considers material properties (f_{Mat} and $xE_{\mathrm{m,min}}$) separate from mill environment described in terms of the impact energy distribution. Consequently, Eq. 7 should have a wide application to various impact milling processes. Toward this effort, determination of the specific breakage rate parameter will be investigated in this study. Although the physical specific breakage rate parameter was derived by first considering the particle breakage model of Vogel and Peukert[9,10] due to its wide use and applicability to a wide variety of materials, similar formulations may originate from other particle-scale breakage models.[33,34] In some cases, such as in milling processes resulting in abrasion or attrition, it would be more appropriate to begin with a breakage model specifically developed for such processes.[34] While comparison between different particle breakage models is outside the scope of this study, physically based particle-scale models should be used in conjunction with particle scale dynamics provided by DEM in efforts to analyze and quantify particle breakage behavior in milling processes.

Methods

Experimental milling

Experimental milling data were taken from a study on the ball milling of silica glass performed by Kotake et al.[35] The study uses a rolling ball mill in which grinding media (alumina beads) and the feed material (silica glass beads) are contained in a cylindrical vessel whose material of construction is alumina. The vessel rotates along its center axis causing the grinding media and feed to rise and fall. The feed particles are fractured if the motion of the grinding media causes sufficiently intense impacts that result in high stresses. Kotake et al.[35] specifically investigated the effect of feed particle size and grinding media size on the breakage rate of the silica glass. Various narrowly distributed feeds of silica glass were processed for a maximum of 5 min and Eq. 4 was fit to the data in which the specific breakage rate parameter k was obtained. This method of determining k will hereafter be referred to as the "experimental method." The experimental details of the mill geometry and operating conditions are listed in Table 1. This study was chosen because the rolling ball mill is frequently studied and simulated using DEM.[17] Kotake et al.[35] had also systematically investigated various grinding media–feed size combinations, which can be simulated in this study to determine the impact energy distribution and specific breakage rate parameter using Eq. 7. The results obtained by simulations can then be compared to the experimentally obtained specific breakage rate parameter to determine the validity of the methods used in this study.

DEM milling simulations

Three-dimensional (3-D) DEM simulations of spheres representing silica glass beads processed in a rolling ball mill (detailed in the previous section) were performed to determine the motion and mechanical interactions between the feed, media, and mill geometry. While the breakage of particles was not simulated, the DEM simulation allows determination of the impact energy distribution for the initial feed condition. The mill geometry was modeled on a 1:1 basis except for the mill length, which was reduced by half as detailed in Table 1. To keep the fractional loading of the

Table 1. Experimental Milling and DEM Simulated Milling Geometry and Operating Specifications

	Experiment[a]	Simulation
Mill diameter	144 mm	144 mm
Mill length	129 mm	64.5 mm
Vessel material	Alumina ($\rho = 4000$ kg/m^3)	Alumina ($\rho = 4000$ kg/m^3)
Mill rotation speed	108 rpm	108 rpm
Grinding media	2 kg Alumina ($\rho = 4000$ kg/m^3)	1 kg Alumina ($\rho = 4000$ kg/m^3)
Grinding media diameter	3–30 mm	3–30 mm
Feed	200 g Silica glass ($\rho = 2150$ kg/m^3)	100 g Silica glass ($\rho = 2150$ kg/m^3)
Feed diameter[b]	1.41–6.7 mm	1.5–6 mm

[a]Experimental study was performed by Kotake et al.[35]
[b]Experimental feeds consist of narrow size distributions whereas simulated feeds are mono sized.

mill constant, media mass and feed mass were accordingly reduced by half. This allows faster computation of the simulations due to the fewer number of particles. Six cases were simulated and compared to experimental results in which five different media sizes and three different feed sized were considered. The media–feed combinations are as follows: 30–3, 20–3, 10–3, 5–3, 30–6, and 3–1.5 mm. Limited by computation power, feed particle sizes finer than 1.5 mm which corresponds to 26,320 particles (44,000 particles total with media) were not simulated. In addition, media and feed particle sizes were modeled on a 1:1 basis compared to experiments. Because reduction of the mill length may have an impact on the motion of particles due to wall effects or axial mixing of the feed, the 30–3 mm experiment was repeated with the full mill length. The specific breakage rate parameter differed by less than 5% showing little effect of the side walls of the mill or effects of axial mixing. Thus, all simulations were performed with half the mill length as specified in Table 1.

In simulations, media and feed were modeled as mono-sized spheres, which were used to approximate the narrow size distributions prepared by Kotake et al.[35] Media and feed particles were randomly generated in the milling vessel and allowed to come to rest. The mill was then rotated and allowed to reach a steady state before data collection began. Steady state was determined by the average particle velocity. Data were collected for every collision associated with the feed for a total of 10 s of simulated time. This includes feed–feed, feed–media, and feed–vessel collisions. Impacts collected for a duration of 20 s (30–3 mm case) did not significantly change the impact energy distribution, thus 10 s was determined to be sufficient to gain an adequate sample size of impacts. Also 10 s results in greater than 90% of the feed left unbroken as determined from experiments.[35] Thus, the impact energy distribution determined by DEM simulation in 10 s should not deviate significantly from the initial condition if breakage were also considered.

Commercial DEM software, EDEM by DEM Solutions, was used to perform the 3-D simulations. While a detailed description of the modeling scheme and numerical methods can be found elsewhere,[16] a short description is given here. DEM resolves the translational and rotational motion of particles integrating Newton's second law of motion. When particles come into contact with either another particle or the vessel geometry, contact mechanic models resolve the force and resultant motion of the interaction. The motion of each particle and the forces acting on every particle is resolved and updated every numerical time-step of the simulation.

The Hertz–Mindlin (no slip) soft particle model was used to resolve particle interactions and was chosen due to its accurate and efficient force calculation. This force model is based on the theory of Hertz[36] and Mindlin.[37] The normal force component F_n shown in Eq. 8 is a function of the normal particle overlap δ_n in which the first term on the r.h.s. is the elastic force and the second is a damping force, which takes into account the coefficient of restitution e

$$F_n = \frac{4}{3}E^*\sqrt{R^*}\delta_n^{3/2} - 2\sqrt{\frac{5}{6}}\frac{\ln e}{\ln^2 e + \pi^2}\sqrt{2E^*m^*}(R^*\delta_n)^{1/4}v_n^{rel} \quad (8)$$

here v_n^{rel} is the normal component of the relative velocity between two particles at contact. The equivalent Young's modulus E^*, equivalent radius R^*, and equivalent mass m^* are defined by Eqs. 9–11 as

$$E^* = \left[\frac{1-v_a^2}{E_a} + \frac{1-v_b^2}{E_b}\right]^{-1} \quad (9)$$

$$R^* = \left[\frac{1}{R_a} + \frac{1}{R_b}\right]^{-1} \quad (10)$$

$$m^* = \left[\frac{1}{m_a} + \frac{1}{m_b}\right]^{-1} \quad (11)$$

Here E, R, m, and v are Young's modulus, radius, mass, and Poisson ratio of a particle "a" in contact with particle "b". The tangential force F_t is modeled by Eq. 12 and is based on the work of Mindlin and Deresiewicz.[38] The tangential force is a function of the tangential particle overlap δ_t in which the first term on the r.h.s. is the elastic force and the second is a damping force

$$F_t = -8G^*\sqrt{R^*\delta_n}\delta_t - 2\sqrt{\frac{5}{6}}\frac{\ln e}{\ln^2 e + \pi^2}\sqrt{8G^*m^*}(R^*\delta_n)^{1/4}v_t^{rel} \quad (12)$$

here G^* is the equivalent shear modulus and calculated form the shear modulus G as shown in Eqs. 13 and 14

$$G^* = \left[\frac{1-v_a^2}{G_a} + \frac{1-v_b^2}{G_b}\right]^{-1} \quad (13)$$

$$G = \frac{E}{2(1+v)} \quad (14)$$

Finally, the rotational motion τ of a particle contacting a surface is determined by Eq. 15

$$\tau_a = -\mu_r F_n R_a \omega_a \quad (15)$$

where μ_r is the coefficient of rolling friction and ω is the angular velocity.

The model parameters used in all simulations are listed in Table 2, except otherwise noted. While parameters are often chosen so that the granular flow or a metric such as power

Table 2. DEM Simulation Parameters for Silica and Alumina

Parameter	Value
Poisson's ratio, v	0.3
Shear modulus, G (Pa)	1×10^7
Coefficient of restitution, e	0.75
Rolling friction coefficient, μ_r	0.02
Sliding friction coefficient, μ_s	0.75
Numerical time step (s)	7.5×10^{-6}

draw match between simulation and experiment, this could not be performed since experiments were not performed in-house. However, ball milling is extensively studied in literature with the materials under investigation here (alumina and silica glass). A typical Poisson's ratio of 0.3 was used, which is valid and commonly selected for most materials. A shear modulus of 1×10^7 Pa was used, which is significantly smaller than the true values for silica and alumina, but does not have an effect on either particle velocities or dissipation energy, which is of concern in this study.[39] In addition, such values of the shear modulus are common to use in similar milling studies in which simulations and experiments were directly compared.[12] While the coefficient of friction can vary widely for both silica and alumina, 0.75 was chosen as a typical value.[40] The coefficient of restitution, e was initially chosen to be 0.75, but is noted as an important parameter for particle interactions in the above set of equations and would have the most effect on simulations, hence was investigated thoroughly in the following. A simulation time-step of 7.5×10^{-6} s was chosen, which is 20% of the Rayleigh time step under consideration of the smallest particle size simulated (1.5 mm). The Rayleigh time step is the time taken for a shear wave to propagate across a particle and is the theoretical maximum, which can accurately calculate particle contact forces.[41]

Determination of the specific breakage rate parameter k

The determination of the specific breakage rate parameter from Eq. 7 requires the impact energy distribution, which is obtained from DEM. The impact energy can be defined by several methods. The most common is the use of the collision energy E_{coll} otherwise known as the kinetic energy at impact given by Eq. 16 where the reduced mass m_R of Eq. 17 is used[23–25]

$$E_{coll} = \frac{1}{2} m_R \left(v_n^{rel}\right)^2 \tag{16}$$

$$m_R = \frac{2 m_a m_b}{m_a + m_b} \tag{17}$$

A second type of impact energy known as the dissipated energy E_d is commonly used in the modeling of impact milling leading to particle fracture.[11,12] This is the energy lost by the inelastic collision of two particles otherwise known as the deformation energy. The dissipated energy is commonly calculated by integrating the normal damping force F_n^d and the tangential damping force F_t^d with respect to their overlaps over the entire contact period $t_{contact}$ as shown in Eq. 18[11,12,42]

$$E_d = \int_0^{t_{contact}} \left(F_n^d d\delta_n + F_t^d d\delta_t\right) \tag{18}$$

The dissipation energy was chosen to define the impact energy distribution after both energies were scrutinized in preliminary DEM simulations as described in the next section. As required by Eq. 7, the mass-specific dissipation energy was used. The dissipated energy was calculated for every collision and placed into $L = 1800$ bins ranging from 1 J downward with a geometric progression ratio of $2^{1/28}$ and $E_{m,1800} = 10^{-20}$ J.

Equation 7 also requires the material properties f_{Mat} and $xE_{m,min}$ to be specified. These parameters can be determined by fitting Eq. 2 to single particle impact tests as described by Vogel and Peukert.[9] In the absence of these experiments, f_{Mat} and $xE_{m,min}$ were identified by fitting Eq. 7, now with the calculated impact energy distribution from DEM simulations, to experimental data. Since these parameters are regarded as material properties and should not vary with milling conditions, the specific breakage rate parameter of the six DEM simulations were simultaneously fit to the six experimentally determined specific breakage rate parameters. This was accomplished by minimizing the sum-of-squared-residual between the theoretical (Eq. 7) and experimental values of k (six total comparisons) using the optimization routine known as "fmincon" of the optimization library of Matlab v 8.0.

Results and Discussion

Defining the impact energy distribution

Determining the impact energy distribution in DEM simulations is critical for accurate determination of the specific breakage rate parameter. The impact energy obtained by DEM is commonly defined by either the collision energy E_{coll} of Eq. 16 or the dissipated energy E_d of Eq. 18. A DEM study of Wang et al.[12] investigated both types of energy in determining the specific breakage rate parameter for a ball milling process and found that both types of impact energy yielded similar results although correction factors were used in each case. Here three particle impact scenarios as depicted in Figure 1 will conclude that dissipation energy should be used to determine the impact energy distribution in subsequent DEM simulations.

Figure 1 depicts three possible scenarios for particle interactions in a DEM simulation for ball milling, which are meant to be illustrative but representative of three out of many possible impact scenarios, which could take place in ball milling. The first scenario (Figure 1a) depicts a 3 mm sphere representing a silica glass bead impacting a stationary 30 mm sphere representing an alumina bead at 1 m/s while the second (Figure 1b) depicts the opposite. The third scenario (Figure 1c) depicts a 30 mm alumina bead impacting a small particle bed (100 total particles) at 1 m/s. If calculating the impact energy as the collision energy, the first two scenarios will yield the same result of 3.04×10^{-5} J since the relative normal velocity and the reduced mass are the same. Yet in calculating the dissipated energy, different results are obtained in each case. The dissipated energy in the first case is 7.12×10^{-6} and 4.50×10^{-3} J in the second separating each other by about three orders of magnitude. The first scenario can be loosely approximated as a feed particle impacting a wall in which case the reduced mass can be defined as the mass of the feed particle yielding a "true" collision energy of 1.52×10^{-5} J. Correspondingly, the collision energy in the first scenario is overestimated by a factor of $\sim$2 due to a larger reduced mass (Eq. 17) while the dissipated energy is lower due to the partially elastic nature of

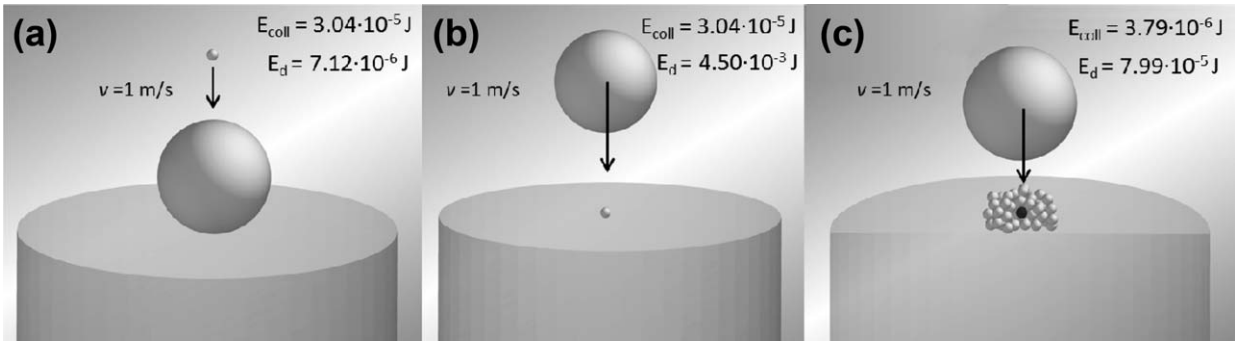

Figure 1. DEM simulations of (a) a 3 mm silica glass particle impacting a 30 mm alumina media particle at 1 m/s, (b) a 30 mm alumina particle impacting a 3 mm silica glass particle at 1 m/s, and (c) a 30 mm alumina media impacting a particle bed at 1 m/s.

Collision energy E_{coll} and dissipation energy E_d are listed in the figure for each scenario. Simulation parameters are listed in Tables 1 and 2.

the particle. Determining impact energy by either collision of dissipation energy cannot be concluded until the second scenario is investigated.

In the second scenario, it would be more appropriate to define the reduced mass as simply the mass of the alumina bead yielding a "true" collision energy of 2.83×10^{-2} J. Comparing the collision energy and the dissipated energy in the second scenario shows that the latter (4.50×10^{-3} J) more closely represents the "true" energy of the collision whereas the collision energy in the original calculation is underestimated by three orders of magnitude (3.04×10^{-5} J). Thus, the collision energy cannot effectively differentiate between the two impact scenarios in part due to the necessity to define a reduced mass, which is sensitive to the mass of the feed particle. Thus, the collision energy may be ambiguous to define depending on the configuration of the impact. Dissipated energy is calculated based on the collision force, which is directly determined by DEM, thus will better differentiate and better represent impacts of different types. On the other hand, collision energy is calculated based on relative velocity and makes no distinction between these two impacts.

The third scenario also emphasizes the deficiencies of using collision energy. If only the dark shaded particle is considered (see Figure 1c), the simulation will register a feed–feed collision since the alumina bead impacting the particle bed is unlikely to contact this particular feed particle. Furthermore, the relative velocities are likely to be small or near zero among the feed particles in the stationary powder bed. This will grossly underestimate the actual energy transmitted to the dark shaded particle by the impacting alumina bead if the collision energy is considered. On the other hand, the energy transmitted from the alumina bead to the particle bed may be determined by the forces transmitted and acting on each particle. Thus, a method that calculates the impact energy directly based on contact forces such as dissipated energy will better represent the impact energy than an indirect method that considers the relative velocities. As shown in Figure 1c, the dissipated energy (7.99×10^{-5} J) is an order of magnitude greater than the collision energy (3.79×10^{-6} J) for the particle under consideration confirming that the energy transmitted from the alumina bead will be underestimated when using the latter due to small relative impact velocities that may result in powder beds. Accordingly, the impact energy distribution for the subsequent DEM simulations of the rolling ball mill will be calculated based on the dissipated energy of Eq. 18.

Rolling ball mill simulations

Spheres representing silica glass beads processed in a rolling ball mill corresponding to the experiments of Kotake et al.[35] were simulated by DEM according to the conditions listed in Tables 1 and 2 to obtain the motion and mechanical interactions between the feed, media, and mill geometry for the initial feed condition. Six different media–feed combinations were simulated as specified in Table 3: 30–3, 20–3, 10–3, 5–3, 30–6, and 3–1.5 mm. The impact energy distribution defined by the dissipation energy along with the

Table 3. DEM Simulation Specifications with Select Results Including the Specific Breakage Rate Parameter Determined by Eq. 7 and Experimentally

Media Size–Feed Size (mm)	Number of Media Particles	Number of Feed Particles	Collision Frequency, $f_{coll} \times 10^{-3}$ (1/s)	Mass-Specific Energy Dissipation Rate,[a] $\dot{E}_{m,d}$ (J/kg s)	Specific Breakage Rate Parameter, k (1/min)	
					DEM Simulation[a]	Experimental[b]
30–3	17	3290	1767	4.25	0.823	0.838
20–3	60	3290	1601	2.07	0.401	0.531
10–3	478	3290	1904	0.66	0.128	0.153
5–3	3820	3290	1554	0.22	0.043	0.034
30–6	17	411	568	1.48	0.572	0.456
3–1.5	17,684	26,320	2246	0.31	0.030	0.028

[a]Determined from optimization with $f_{Mat} = 1.08$ kg/J·m and $xE_{m,min} = 2.97 \times 10^{-3}$ J·m/kg.
[b]Experimental study was performed by Kotake et al.[35]

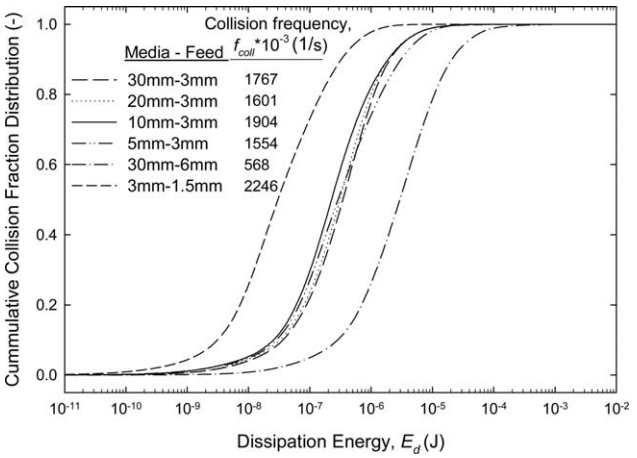

Figure 2. Impact energy distribution using the dissipated energy E_d obtained from DEM simulations corresponding to the conditions listed in Tables 1–3.

Collision frequency is listed in the figure. The distributions pertain only to impacts involving a feed particle.

collision frequency f_{coll} is shown in Figure 2 for the six simulations. Furthermore, these impacts pertain only to those experienced by the feed by means of feed–feed, feed–media, and feed–vessel type interactions. The impact energy distribution shows that the most energetic collisions are obtained for the 6 mm feed particles milled with the 30 mm media. The collision frequency that was averaged over the 10 s of collection time (568×10^3 1/s) is the lowest since this simulation contains the fewest number of feed particles (411) for which collisions to occur by feed–feed, feed–media, and feed–vessel type impacts. The least energetic impacts are shown for the 1.5 mm feed milled with the 3-mm media, which is expected given the low mass of the individual particles relative to the other milling experiments. The collision frequency (2246×10^3 1/s) is also the highest in this case given the large number of feed particles (26,320). The simulations corresponding to the 3 mm feed particles show impacts of an intermediate energy and collision frequency ($\sim$1600–1900 $\times 10^3$ 1/s). Interestingly, the impact energy distribution and impact frequency appear to be similar for all four cases using media sizes of 30, 20, 10, or 5 mm. This is unexpected since larger and more massive media should result in more energetic impacts.

To investigate this observation, the impact frequencies of the most energetic collisions ($>1 \times 10^{-6}$ J) which account for $\sim$20% of the total impacts were scrutinized further as shown in Figure 3. Figure 3 (top) shows that the largest media size of 30 mm indeed does produce the most energetic impacts as high as 5×10^{-3} J, whereas the small media size of 5 mm fail to produce impacts larger than 1×10^{-4} J. Media sizes of 10 and 20 mm produce impacts of an intermediate range as would be their expected trend. According to the impact energy distribution of Figure 2, these impacts and particularly those greater than 1×10^{-5} J only account for a small fraction of the total number of impacts and thus fail to appear clearly in the cumulative distribution due to the contribution of a large number of low energy collisions. Although these high energy impacts only account for a small number of the total impacts, they also appear to be the most important for breakage considering that the frequency of impacts with energy $>1 \times 10^{-5}$ J are the most differentiating feature of the impact energy distributions for the 3 mm feed simulations, which are known to have significant differences in the experimental specific breakage rate parameters (see Table 3). It is then reasonable to infer that the majority of the impacts are likely those which do not contribute to breakage. This is more fully investigated in the subsequent analysis below and in the next section. Figure 3 (bottom) also shows the impact frequencies for the most energetic collisions ($> 1 \times 10^{-6}$ J) for the experiments 30–6 and 1.5–3 mm. As expected, the most energetic impacts are observed for the former case, whereas the latter case contains the least energetic collisions.

Taking the impact energy distributions of Figure 2, the specific breakage rate parameter of Eq. 7 was determined for the six simulated cases using f_{Mat} and $xE_{m,min}$ as fitting parameters. The values of $f_{Mat} = 1.08$ kg/J·m and $xE_{m,min} = 2.97 \times 10^{-3}$ J·m/kg resulted in the best fit (lowest sum-of-squared residual) of the theoretical specific breakage rate parameter to the experimental values (Kotake et al.[35]), which are in close approximation as shown in Figure 4 and Table 3. Since one set of values for f_{Mat} and $xE_{m,min}$ were successful in determining the specific breakage rate parameter for six different milling conditions, they are confirmed to be material-dependent properties as described by Vogel and Peukert.[9,10] This set of parameters may potentially be used

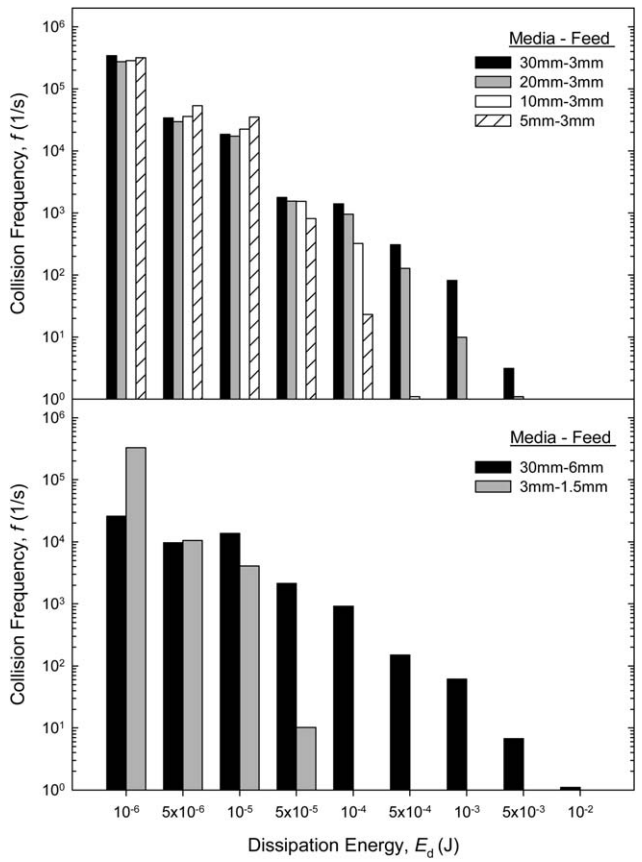

Figure 3. Collision frequency for dissipation energy E_d greater than 1×10^{-6} J obtained from DEM simulations corresponding to the conditions listed in Tables 1–3.

The distributions pertain only to impacts involving a feed particle.

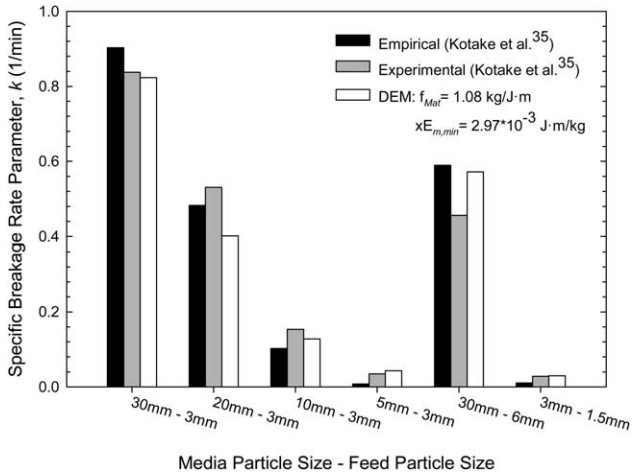

Figure 4. Comparisons between the specific breakage rate parameter *k* determined by DEM simulations and Eq. 7, experimentally by Kotake et al.,[35] and by the empirical equation of Kotake et al.[35]

with Eq. 7 and the impact energy distribution obtained from DEM to determine the specific breakage rate parameter for any milling condition. Taking the size-independent threshold energy $xE_{\mathrm{m,min}}$ and the impact energy distribution, observations in the experimental breakage rates can be explained. The size-independent energy threshold determined above ($xE_{\mathrm{m,min}}$) corresponds to a minimum impact energy ($E_{\mathrm{m,min}}$) of 7.52×10^{-6}, 3.00×10^{-5}, and 1.20×10^{-4} J for 1.5, 3, and 6 mm feed particles, respectively. Comparing the minimum impact energy to the impact distributions of Figures 2 and 3, it is indeed the higher energy impacts seen in Figure 3 that are responsible for breakage, whereas the majority of impacts seen in Figure 2 are of lower energy below the threshold energy and do not contribute to particle breakage. In addition, the high energy impacts of Figure 3 are the most differentiating feature of the impact energy distributions for experiments using 3 mm feed particles thus explaining the strong dependence of the specific breakage rate parameter on grinding media size. While the experiment of 6 mm feed also contains high energy impacts, the higher minimum energy threshold and lower collision frequency explain the lower specific breakage rate parameter than that of 3 mm feed milled with 30 mm media.

Figure 4 also shows the specific breakage rate parameter as determined by an empirical equation (five total parameters) that Kotake et al.[35] developed specifically to describe the influence of feed and media particle size for these set of experiments. In all cases but one (20–3 mm) the specific breakage rate parameter determined by DEM is in better approximation to the experimental values than the empirical expression. This comparison is meant to demonstrate the superior capability of the physically based specific breakage rate parameter coupled with DEM, which can be potentially used for all milling conditions and milling types. The empirical expression, which includes no physical basis for particle breakage, has limited applicability beyond this set of experiments.

Analysis of impact energy

Since the specific breakage rate parameter is defined based on impact energy, further analysis was performed to closely examine the influence of milling conditions on the energy contributing to particle breakage. Figure 5 shows the separate energy contributions of feed–feed, feed–media, and feed–vessel type impacts for the six simulated milling experiments. Figure 5 (top) assumes that all impacts contribute to breakage ($xE_{\mathrm{m,min}} = 0$ J·m/kg) while Figure 5 (bottom) assumes that only impacts above an energy threshold ($xE_{\mathrm{m,min}} = 2.97 \times 10^{-3}$ J·m/kg) as determined in the previous section contribute to breakage. Thus, the former case gives the total impact energy (contributing + noncontributing) while the latter case is referred to as contributing energy. Furthermore, the energy considered in Figure 5 is the mass-specific dissipation energy rate $\dot{E}_{\mathrm{m,d}}$ or $\sum_{l=1}^{L} f_{\mathrm{coll},l}(E_{\mathrm{m},l} - E_{\mathrm{m,min}})$, which is taken from Eq. 7. Figure 5 (top) shows that feed–feed impacts are the most significant contributors to impact energy for all cases while Figure 5 (bottom) disproves this notion. Feed–feed impacts, while numerous, are characterized by low impact energy and are not actually significant contributors to breakage. When considering only impacts that contribute to breakage [Figure 5 (bottom)], feed–media impacts are indeed the most significant as would be expected since they have the greatest mass and would transmit the most energy and highest stresses during impact. In experiments using small media sizes such as 5 or 3 mm, a significant portion of their impact energy is observed to be wasted or noncontributing as well. Overall, it is evident from such analysis that a significant amount of energy is wasted during ball milling; thus corroborating the

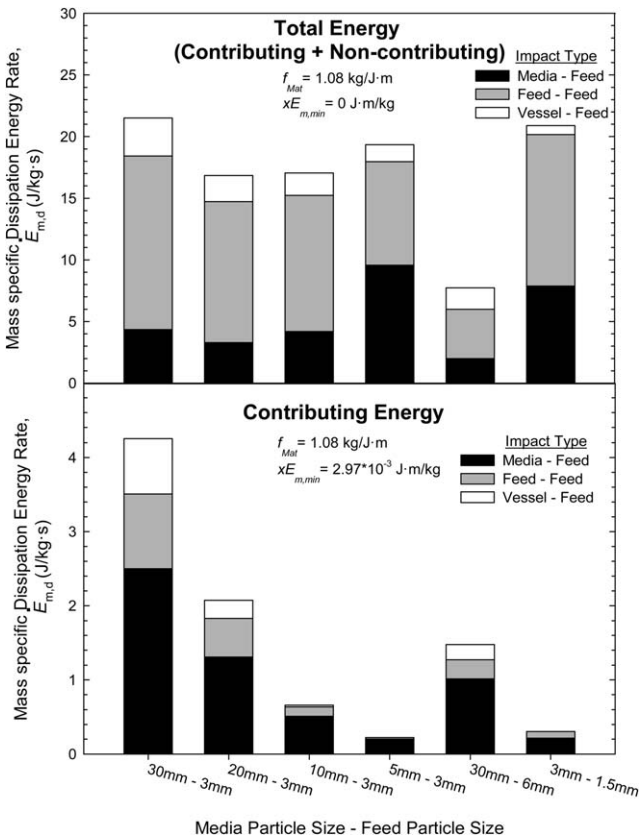

Figure 5. Impact energy contribution of media–feed, feed–feed, and vessel–feed type impacts considering impacts of all energies (top) and impact energy above the threshold xE_{min} (bottom).

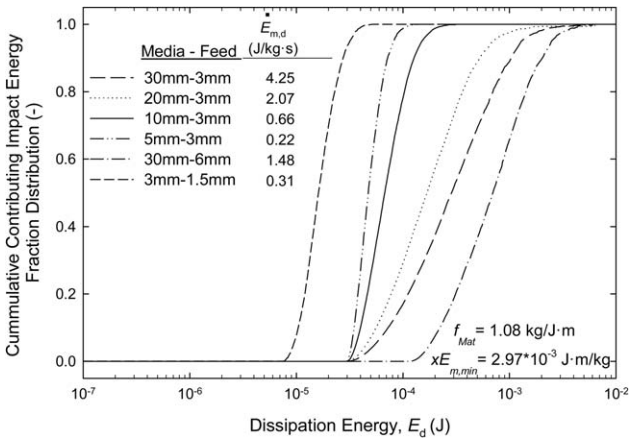

Figure 6. Impact energy distribution referring to the cumulative dissipation energy only for impacts contributing to breakage ($E_{m,d} > xE_{m,min}$).

Mass-specific dissipation energy rate $\dot{E}_{m,d}$ is listed in the figure.

well known fact that energy utilization is very poor in milling processes.[43]

The effect of media size on 3 mm feed particles is also quite interesting. Feed–feed impacts contribute more to particle breakage when processed with large media sizes as can be seen in Figure 5 top and bottom. 7.2, 4.6, 1.1, and 0.2% of the total impact energy due to feed–feed impacts contributes to breakage for 30, 20, 10, and 5 mm media, respectively. This is due to the fact that media cause breakage due to direct feed–media impacts and, in addition, may also transmit energy to the powder bed causing indirect breakage. 30 mm media impacting a powder bed can transmit enough energy to cause feed–feed impacts sufficient for breakage. Conversely, 5 mm media particle cannot, thus feed–feed impacts are rather insignificant for this case. Overall, a large percentage of the energy due to feed–feed is not used toward breakage. Feed–vessel impacts are also the smallest contributors to particle breakage. This is particularly true for the case of 5 mm media particles, which is likely due to the large number of media particle preventing such impacts.

This section emphasizes the importance of analyzing the impact energy distribution within context of a physically based specific breakage rate parameter formulated in this study. If an energy threshold is not considered, the specific breakage rate parameter, which is calculated based on the impact energy rate ($k=f_{Mat}x\dot{E}_{m,d}$), can be grossly miscalculated as seen in the high impact energy dissipation rates of Figure 5 (top) as compared to Figure 5 (bottom). This section also establishes that collisions which contribute the most to the impact energy may not contribute to the actual breakage of particles as seen by the large number of collisions below the threshold energy. Figure 6 shows the cumulative energy contribution of impacts with respect to dissipation energy and only include impacts, which contribute to particle breakage ($E_m > E_{m,min}$). This figure is meant to be a complementary figure to the cumulative collision fraction distribution of Figure 2. Whereas Figure 2 shows that low energy collisions dominate the collision number distribution, Figure 6 shows that a relatively few number of higher energy impacts are actually responsible for the energy contributing to breakage. Thus, previous studies that base their analysis on average or total energy may be misleading.[15,22–25] Future attempts to determine milling performance from particle interactions should carefully consider the issues discussed here.

Effect of coefficient of restitution, e

The specific breakage rate parameters determined in previous sections were in good agreement with experimental results lending credibility to the parameters chosen for DEM simulations. However, DEM simulations are often validated against experiments based on a qualitative comparison with granular flow or between simulated and experimental power draw.[11,12] Ideally, the coefficient of restitution and other DEM parameters such as friction coefficients would be determined experimentally.[42,44] Since experiments were taken from literature,[35] direct comparisons could not be made, and hence the selection of the coefficient of restitution could not be validated in that manner. Although the specific breakage rate parameters were in good agreement as stated before, examining the influence of the coefficient of restitution is warranted and although not intended to be used as a "fitting parameter" it was varied in this section because it is an important parameter for particle interactions. It is noted that the coefficient of restitution also specifies the damping coefficient, which is used to calculate the damping force and dissipated energy.

Simulations were repeated for the six experiments with only a difference in the coefficient of restitution, which was varied from 0.05 to 0.95. f_{Mat} and $xE_{m,min}$ were again determined by the fitting procedure and are shown in Figure 7 along with the sum-of-squared residual in Figure 8. A coefficient of restitution of 0.75 yielded the best fit (lowest sum-squared residual) confirming the best choice of coefficient of restitution, which was used in the previous analysis. Decent fits could also be obtained with a coefficient of restitution of 0.35 and 0.55, which also yield similar values of f_{Mat}, though $xE_{m,min}$ appears to be more sensitive to coefficient of restitution. While the coefficient of restitution can vary widely, 0.7 has previously been used for alumina in DEM milling studies although 0.9 is also common for glass.[45] Hence 0.75 that was chosen for both materials in the previous discussion seems reasonable. While it may be possible that the actual coefficient of restitution for the materials used in this study may deviate slightly, it should be stressed that the results

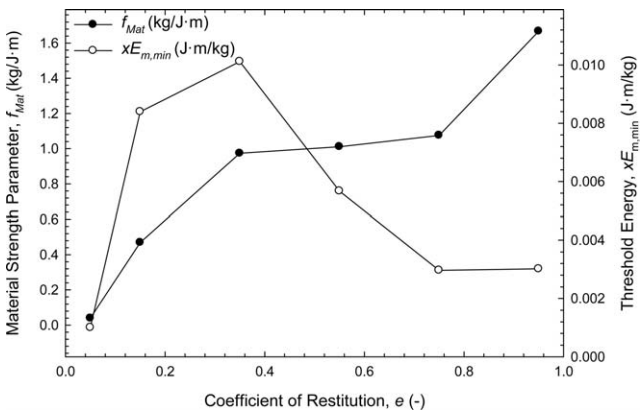

Figure 7. Material strength parameter f_{Mat} and size-independent threshold energy $xE_{m,min}$ for various values of the coefficient of restitution used in DEM simulations.

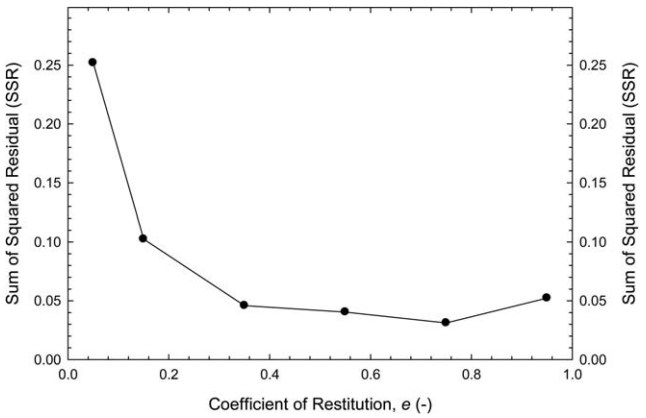

Figure 8. Sum of squared residual between the experimental and the theoretical specific breakage rate parameter using the material strength parameter f_{Mat} and size-independent threshold energy $xE_{m,min}$ shown in Figure 7.

and major conclusions found in the previous section would not have changed specifically with regards to the analysis of the milling process under consideration of an impact energy threshold within the context of the physical based specific breakage rate parameter.

The values for f_{Mat} and $xE_{m,min}$ can be compared to those obtained by Vogel and Peukert[9] in single particle breakage tests for glass in which they found values of 0.945 kg/J·m and 0.1 J·m/kg, respectively. The value for f_{Mat} determined for a coefficient of restitution of 0.75 is similar with a value of 1.08 kg/J·m providing further credence to the methods used in this study. The value of $xE_{m,min}$ determined for a coefficient of restitution of 0.75, however, was 2.97×10^{-3} J·m/kg, which is lower by about 30 times than that determined by single particle impact tests. The possible discrepancy may be partly due to the method Vogel and Peukert[9] used to find the threshold energy. Vogel and Peukert[9] plotted breakage probability as a function of impact energy and extrapolated to the energy at which breakage probability is zero, which is assumed to be the threshold energy. It is possible that the threshold energy is lower than what can be found by simple extrapolation and that significantly smaller energies when accumulated can result in particle breakage. Another possible reason may be the different grades of silica glass used which was not specified in either study and cannot be verified at this time. Lastly, possible discrepancy between f_{Mat} and $xE_{m,min}$ may be due to differences in the impact energy defined by DEM through dissipation energy with those defined by Vogel and Peukert[9,10] in single particle impact tests. Although the specific breakage rate parameter determined by DEM agrees with the experiment, which suggests that impact energy distributions are accurate, it is unknown how dissipation energy relates to the experimentally defined impact energy. This would not invalidate the proposed methods in this study or alter the physical meaning of f_{Mat} and $xE_{m,min}$ as material parameters, but it may prevent f_{Mat} and $xE_{m,min}$ being used interchangeably between single particle impact experiments and DEM simulations. Further fundamental work needs to be carried out using a combined approach of DEM simulations and single particle or particle bed impact tests to determine the accuracy of impact energy distributions as well as the use of ultrafast load cells[46] to determine fracture energies more accurately.

Conclusions and Future Perspective

This article aimed to develop a method to use particle scale interactions to quantify milling performance for batch dry milling processes. A physically motivated specific breakage rate parameter was derived, which explicitly considers the impact energy distribution obtained from DEM simulations. Furthermore, the specific breakage rate parameter used here effectively separates material properties (f_{Mat} and $xE_{m,min}$) from effects of the milling environment, which may offer greater applicability to a wide range of milling processes. In addition to concluding that dissipation energy (E_d) should be used in contrast to collision energy (E_{coll}) to define the impact energy distribution, this study took a more thorough analysis of the data. Results show that a threshold energy must be considered to determine the impact energy that contributes to breakage. If a threshold value is not considered, a large number of small energy impacts, which do not contribute to particle breakage may lead to erroneous interpretation of the milling simulation. Such fundamental analysis is only feasible in context of the physically based specific breakage rate parameter derived in this study and should lead to superior examination of milling processes. Finally, DEM simulations corresponding to the initial condition of the experimental ball milling of silica glass were performed to determine the specific breakage rate parameter for various feed and media particle sizes. Comparison to specific breakage rate parameters determined by experiments[35] showed good agreement validating the methods developed in this study. While the main novelty of this study involved formulation of a physical specific breakage rate parameter of the PBM for batch milling within context of the particle breakage model of Vogel and Peukert,[9,10] integration of different particle–scale breakage models for fracture[33] or attrition[34] may be possible using the methodology presented here.

While the results of this study were limited to mono-sized particles, determination of the specific breakage rate parameter is traditionally determined experimentally by such feeds. Thus, the methods put forth here should be directly amenable with current experimental practices, which are used to calculate the specific breakage rate parameter and ultimately the breakage rate and the PSD from the PBM of Eq. 1. Future work will focus on extending the methodology to polydispersed feeds, which in addition to being more representative of actual feeds, should also reduce the number of experiments by determining the specific breakage rate parameter for all particle sizes simultaneously as opposed to a large number of mono-size feed experiments.

Extension of these methods to polydispersed feeds should also aid in the elucidation of processes, which display nonlinear breakage kinetics. Many dense-phase dry milling processes deviate from first-order breakage kinetics as assumed by the PBM of Eq. 1 and are difficult to model.[47,48] Non-first-order or nonlinear breakage kinetics originate due to temporal variation of the mechanical interactions among particles in the evolving population density.[47] Thus, the specific breakage rate parameter of a particle is generally dependent on the instantaneous PSD. DEM, which provides particle scale interactions, combined with the physically based specific breakage rate parameter should allow better fundamental analysis of milling processes, which display nonlinear breakage kinetics. Ultimately, such an approach

should improve the design, control, and optimization of milling processes.

Acknowledgment

The authors acknowledge financial support from the National Science Foundation Engineering Research Center for Structured Organic Particulate Systems (NSF ERC for SOPS) through the Grant EEC-0540855.

Literature Cited

1. Prasher C. *Crushing and Grinding Process Handbook*. Chichester: Wiley, 1987.
2. Austin L. A review: introduction to the mathematical description of grinding as a rate process. *Powder Technol.* 1971;5:1–17.
3. Hennart S. Identification of the grinding mechanism and their origin in a stirred ball mill using population balances. *Chem Eng Sci*. 2009; 64:4123–4130.
4. Randolph A, Larson M. *Theory of Particulate Processes*. San Diego: Academic Press, 1988.
5. Austin L, Bhatia V. Experimental methods for grinding studies in laboratory mills. *Powder Technol.* 1972;5:261–266.
6. Austin L, Luckie P. Methods for determination of breakage distribution parameters. *Powder Technol.* 1972;5:215–222.
7. Capece M, Bilgili E, Dave R. Identification of the breakage rate and distribution parameters in a non-linear population balance model for batch milling. *Powder Technol.* 2011;208:195–204.
8. Klimpel R, Austin L. The back-calculation of specific rates of breakage and non-normalized breakage distribution parameters from batch grinding data. *Int J Miner Process*. 1977;4:7–32.
9. Vogel L, Peukert W. Breakage behaviour of different materials—construction of a mastercurve for the breakage probability. *Powder Technol*. 2003;129:101–110.
10. Vogel L, Peukert W. From single particle impact behaviour to modelling of impact mills. *Chem Eng Sci*. 2005;60:5164–5176.
11. Datta A, Rajamani R. A direct approach of modeling batch grinding in ball mills using population balance principles and impact energy distribution. *Int J Miner Process*. 2002;64:181–200.
12. Wang M, Yang R, Yu A. DEM investigation of energy distribution and particle breakage in tumbling ball mills. *Powder Technol*. 2012; 223:83–91.
13. Tavares L, Carvalho R. Modeling breakage rate of coarse particles in ball mills. *Miner Eng*. 2009;22:650–659.
14. Lee H, Cho H, Kwon J. Using the discrete element method to analyze the breakage rate in a centrifugal/vibration mill. *Powder Technol*. 2010;198:364–372.
15. Concas A, Lai N, Pisu M, Cao G. Modelling of comminution processes in Spex mixer/mill. *Chem Eng Sci*. 2006;61:3746–3760.
16. Cundall P, Strack O. A discrete numerical model for granular assemblies. *Geotechnique*. 1979;29:47–65.
17. Zhu H, Zhou Z, Yang R, Yu A. Discrete particle simulation of particulate systems: theoretical developments. *Chem Eng Sci*. 2007;62: 3378–3396.
18. Mishra B. A review of computer simulation of tumbling mills by the discrete element method: part I—contact mechanics. *Int J Miner Process*. 2003;71:73–93.
19. Zhu H, Zhou Z, Yang R, Yu A. Discrete particle simulation of particulate systems: a review of major applications and findings. *Chem Eng Sci*. 2008;63:5728–5770.
20. Mishra B. A review of computer simulation of tumbling mills by the discrete element method part II—practical applications. *Int J Miner Process*. 2003;71:95–112.
21. Ketterhagen W, Ende M, Hancock B. Process modeling in the pharmaceutical industry using the discrete element method. *J Pharm Sci*. 2009;98:442–470.
22. Hoyer D. The discrete element method for fine grinding scale-up in Hicom mills. *Powder Technol*. 1999;105:250–256.
23. Kwan C, Mio H, Chen Y, Ding Y, Saito F, Papadopoulos D, Bentham A, Ghadiri M. Analysis of the milling rate of pharmaceutical powders using the distinct element method (DEM). *Chem Eng Sci*. 2005;60:1441–1448.
24. Mori H, Mio H, Kano K, Saito F. Ball mill simulation in wet grinding using a tumbling mill and its correlation to grinding rate. *Powder Technol*. 2004;143–144:230–239.
25. Kano J, Saito F. Correlation of powder characteristics of talc during planetary ball milling with the impact energy of the balls simulated by the particle element method. *Powder Technol*. 1998;98:166–170.
26. Bruchmuller J, van Wachem B, Gu S, Luo K. Modelling discrete fragmentation of brittle particles. *Powder Technol*. 2011;208:731–739.
27. Bwalya M, Moys M, Hinde A. The use of the discrete element method and fracture mechanics to improve grinding rate prediction. *Miner Eng*. 2001;16:565–573.
28. Naik S, Malla R, Shaw M, Chaudhuri B. Investigation of comminution in a Wiley mill: experiments and DEM simulations. *Powder Technol*. 2013;237:338–354.
29. Rumpf H. Physical aspects of comminution and a new formulation of a law of comminution. *Powder Technol*. 1973;7:145–159.
30. Bilgili E, Capece M. Quantitative analysis of multi-particle interactions during particle breakage: a discrete non-linear population balance framework. *Powder Technol*. 2011;213:162–173.
31. Bilgili E, Capece M. A rigorous breakage matrix methodology for characterization of multi-particle interactions in dense-phase particle breakage. *Chem Eng Res Des*. 2012;90:1177–1188.
32. Vervoorn P, Austin L. The analysis of repeated breakage events as an equivalent rate process. *Powder Technol*. 1990;63:141–147.
33. Kwan C, Chen Y, Ding Y, Papadopoulos D, Bentham A, Ghadiri M. Development of a novel approach towards predicting the milling behavior of pharmaceutical powders. *Eur J Pharm Sci*. 2004;23:327–336.
34. Ghadiri M, Zhang Z. Impact attrition of particulate solids. Part 1: a theoretical model of chipping. *Chem Eng Sci*. 2002;57:3659–3669.
35. Kotake N, Suzuki N, Asahi S, Kanda Y. Experimental study on the grinding rate constant of solid materials in a ball mill. *Powder Technol*. 2002;122:101–108.
36. Hertz H. On the contact of elastic solids. *J reine und angewandte-Mathematik*. 1882;92:156–171.
37. Mindlin R. Compliance of elastic bodies in contact. *J Appl Mech*. 1949;16:259–268.
38. Mindlin R, Deresiewicz H. Elastic spheres in contact under varying oblique forces. *J Appl Mech*. 1953;20:327–344.
39. Malone K, Xu B. Determination of contact parameters for discrete element method simulations of granular systems. *Particuology*. 2008;6:521–528.
40. Jahanmir S. *Friction and Wear of Ceramics*. New York: Marcel Dekker, 1994.
41. Yanjie L, Yong X, Thornton C. A comparison of discrete element simulations and experiments for 'sandpiles' composed of spherical particles. *Powder Technol*. 2005;160:219–228.
42. Santhanam P, Dreizin E. Predicting conditions for scaled-up manufacturing of materials prepared by ball milling. *Powder Technol*. 2012;221:403–411.
43. Coulson J, Richardson J, Backhurst J, Harker J. *Size Reduction of Solids*. Oxford: Butterworth-Heinemann, 1996.
44. Ward T, Chen W, Schoenitz M, Dave R, Dreizin E. A study of mechanical alloying processes using reactive milling and discrete element modeling. *Acta Mater*. 2005;53:2909–2918.
45. Rosenkranz S, Breitung-Faes S, Kwade A. Experimental investigations and modeling of the ball motion in planetary ball mills. *Powder Technol*. 2011;212:224–230.
46. Tuzcu E, Dhawan N, Rajamani R. Coarse particle fracture with ultrafast load cell. *Miner Metall Process*. 2011;28:176–186.
47. Bilgili E, Scarlett B. Population balance modeling of non-linear effects in milling processes. *Powder Technol*. 2005;153:59–71.
48. Austin L, Bagga P. An analysis of fine dry grinding in ball mills. *Powder Technol*. 1981;28,83–90.

Manuscript received Jun. 26, 2013, and revision received Feb. 9, 2014.